http://pubs.acs.org/journal/acsodf
Article

# Rhodamine-Based Fluorescent Probe for Highly Selective Determination of $Hg^{2+}$

Nannan Zhu, Junhong Xu, Qiujuan Ma,* Yang Geng,* Linke Li, Shuzhen Liu, Shuangyu Liu, and Gege Wang

Cite This: ACS Omega 2022, 7, 29236−29245
Read Online

ACCESS | Metrics & More | Article Recommendations | Supporting Information

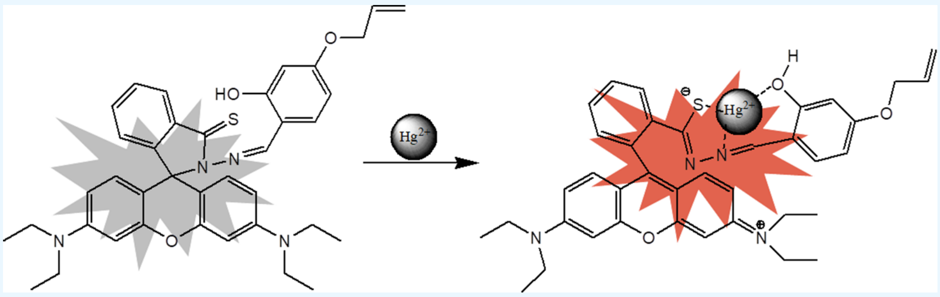


**ABSTRACT:** The determination of mercuric ions ($Hg^{2+}$) in environmental and biological samples has attracted the attention of researchers lately. In the present work, a novel turn-on $Hg^{2+}$ fluorescent probe utilizing a rhodamine derivative had been constructed and prepared. The probe could highly sensitively and selectively sense $Hg^{2+}$. In the presence of excessive $Hg^{2+}$, the probe displayed about 52-fold fluorescence enhancement in 50% $H_2O/CH_3CH_2OH$ (pH, 7.24). In the meantime, the colorless solution of the probe turned pink upon adding $Hg^{2+}$. Upon adding mercuric ions, the probe interacted with $Hg^{2+}$ and formed a 1:1 coordination complex, which had been the basis for recognizing $Hg^{2+}$. The probe displayed reversible dual colorimetric and fluorescence sensing of $Hg^{2+}$ because rhodamine's spirolactam ring opened upon adding $Hg^{2+}$. The analytical performances of the probe for sensing $Hg^{2+}$ were also studied. When the $Hg^{2+}$ concentration was altered in the range of $8.0 \times 10^{-8}$ to $1.0 \times 10^{-5}$ mol $L^{-1}$, the fluorescence intensity showed an excellent linear correlation with $Hg^{2+}$ concentration. A detection limit of $3.0 \times 10^{-8}$ mol $L^{-1}$ had been achieved. Moreover, $Hg^{2+}$ in the water environment and A549 cells could be successfully sensed by the proposed probe.

## INTRODUCTION

Recently, developing highly selective and sensitive sensors for toxic metal ions have been in demand in environmental and biological studies.[1−3] Heavy metal mercury is toxic and bio-accumulating, can be generated by both natural resources and anthropogenic activities, and ubiquitously exists in the global environment. Mercury includes elemental mercury, inorganic mercury, and organic mercury. Mercuric ions ($Hg^{2+}$) are much more common than mercurous ions ($Hg^{+}$), and low-dose $Hg^{2+}$ in the body could cause long-standing irreversible harm to the human health.[4,5] Methylmercury is a dominant form of organic mercury and could be produced through microbiological transformation of $Hg^{2+}$ in the aquatic environment. Moreover, methylmercury could bio-accumulate in the human body by biological food chain and result in a variety of illnesses including cardiovascular diseases, Minamata disease, growth retardation, dyskinesia, and so forth.[6−9] The maximum amount of $Hg^{2+}$ allowed in drinking water is 2 ppb ($10^{-8}$ mol $L^{-1}$) according to the US Environmental Protection Agency.[10] Thus, sensing $Hg^{2+}$ has high significance in environmental and medical science.

To date, many analytic approaches have been employed for sensing $Hg^{2+}$ such as high-performance liquid chromatography−inductively coupled plasma mass spectrometry (HPLC−ICP-MS),[11] HPLC coupled with atomic fluorescence spectrometry (HPLC−AFS),[12] ICP-atomic emission spectrometry (ICP-AES),[13] atomic absorption spectrometry (AAS),[14] ultraviolet−visible absorption spectrometry (UV−vis),[15] fluorometry,[16,17] electrochemical methods,[18,19] and so on. Among all the methods developed, fluorometry possess remarkable advantages because of its high sensitivity, inherent simplicity, instrument operability, in situ detection, and bioimaging analysis in vivo.[16,17] Hitherto, many fluorescent probes had been constructed to determine $Hg^{2+}$.[20−30] However, some analytical performances of these probes are unsatisfactory, including the slow response time,[20−23] cross

Received: May 28, 2022
Accepted: August 2, 2022
Published: August 10, 2022





https://doi.org/10.1021/acsomega.2c03336
ACS Omega 2022, 7, 29236−29245

Scheme 1. Preparation of Fluorescent Probe 1: (a) Hydrazine Monohydrate (85%), $CH_3CH_2OH$, Reflux, 12 h, 86%; (b) Lawesson's Reagent, Toluene, Reflux, 4 h, 17%; (c) Allyl Bromide, Sodium Bicarbonate, Dormyl Dimethylamine, 70 °C, 48 h, 61%; and (d) $CH_3CH_2OH$, Reflux, 12 h, 75%

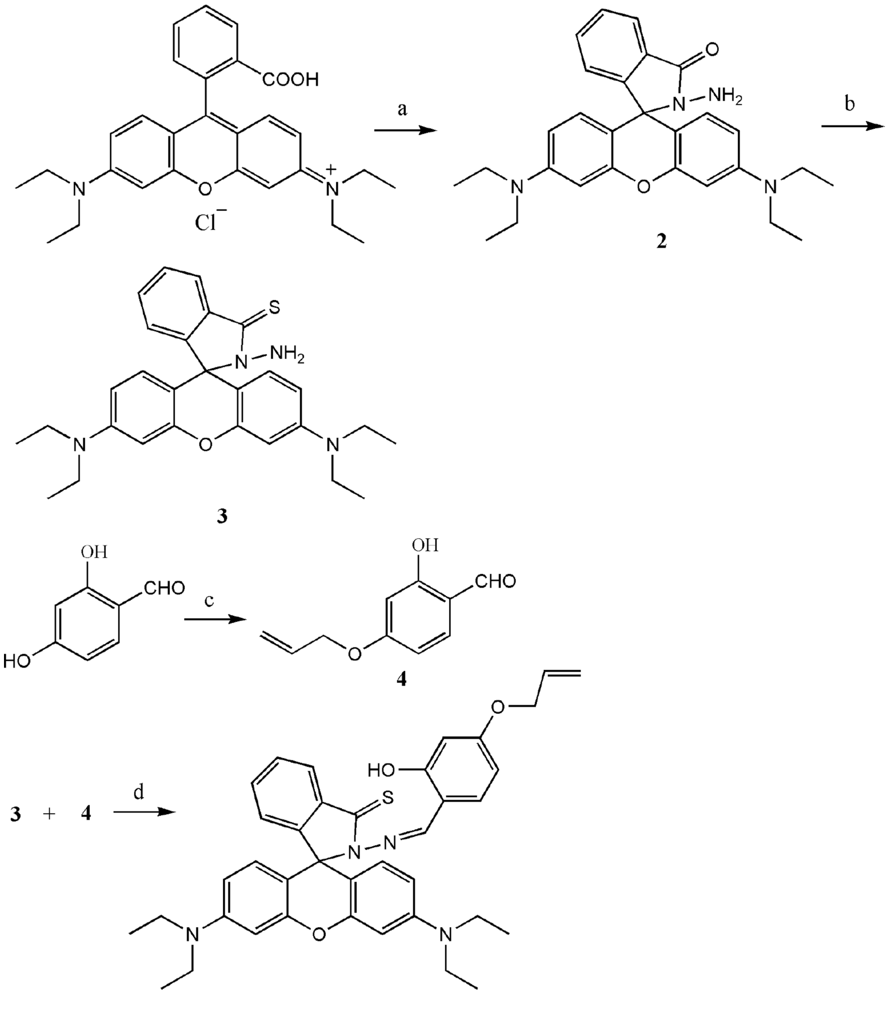


interference,[24,25] poor sensitivity,[26−29] and so forth. Therefore, novel $Hg^{2+}$ fluorescent probes are still desirable, which possess fast response speed, excellent selectivity, and sensitivity.

Rhodamine and rhodamine derivatives have been applied widely as fluorescent probes owing to their remarkable optical characteristics including a high fluorescence quantum yield (Φ), a large molar extinction coefficient ($\varepsilon$), and longer excitation and emission wavelengths.[31] So far, many fluorescent probes utilizing rhodamine derivatives had been utilized to sense different cations including $Cu^{2+}$,[32] $Pb^{2+}$,[33] $Cr^{3+}$,[34] $Fe^{3+}$,[35] $Al^{3+}$,[36] $Zn^{2+}$,[37] and so forth. The sensing mechanism of these probes for cations is based on the transformation from a spirocyclic form into an open cyclic structure. In the absence of cations, these probes displayed no fluorescence and colorlessness because of their spirocyclic form. After adding cations, these probes emitted a powerful fluorescence and showed a pink color because the cyclic structure of the spirolactam or spirolactone was opened through a reversible complexation or nonreversible chemical interaction. The above sensing mechanism has also been applied to construct rhodamine-based $Hg^{2+}$ fluorescent probes.[38−47] However, there are still more or less limitations for some of these $Hg^{2+}$ fluorescent probes including the delayed response,[38] a narrow pH range,[39] and cross interference.[40−44] Thus, developing unusual rhodamine-based fluorescent probes for $Hg^{2+}$ is still very important.

Herein, a new $Hg^{2+}$ fluorescent probe **1** (Scheme 1) had been constructed, which chose rhodamine as the fluorophore. Because sulfur had strong affinity for $Hg^{2+}$,[39,48] we introduced a sulfur-based functional unit to the probe in the present article. To prepare an optical chemical sensor (optode) for $Hg^{2+}$ in the next work, a terminal double bond was included in probe **1** to allow the probe to covalently immobilize on the activated surface of glass slides with the double bond by UV irradiation. When $Hg^{2+}$ was absent, the probe existed in a spirocyclic form and exhibited no fluorescence and colorlessness. When $Hg^{2+}$ was present, the probe emitted yellowish-red fluorescence, and the solution color changed to pink. The $Hg^{2+}$ probe exhibited excellent sensing performances including a fast response time, excellent sensitivity and selectivity, a broad pH working range, and so forth. In addition, nearly no cytotoxic reaction was found, and the probe could be successfully utilized to image $Hg^{2+}$ in A549 cells. Besides, the developed probe was also magnificently utilized to monitor $Hg^{2+}$ in water environments.


https://doi.org/10.1021/acsomega.2c03336
ACS Omega 2022, 7, 29236−29245

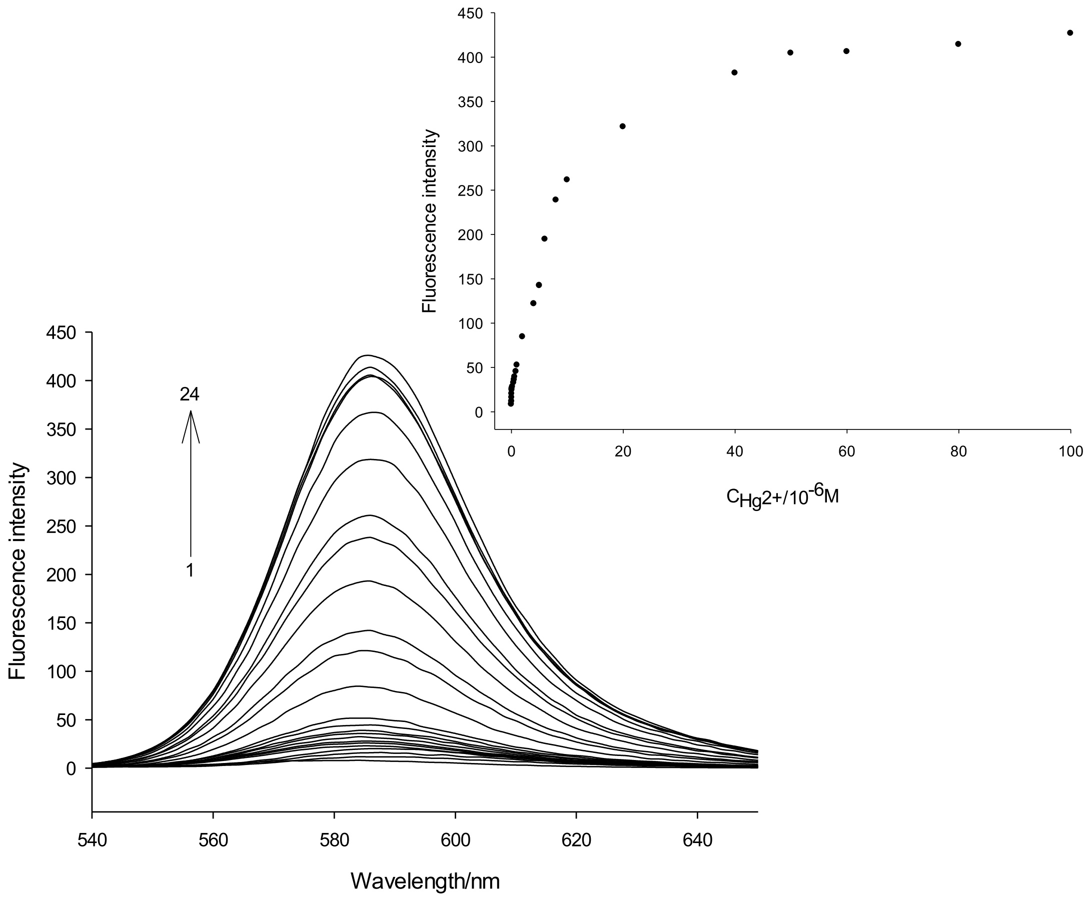


**Figure 1.** Fluorescence spectra of 5.0 $\mu$M probe **1** in the presence of different concentrations of $Hg^{2+}$: 0, 0.03, 0.05, 0.07, 0.08, 0.10, 0.20, 0.40, 0.50, 0.60, 0.80, 1.0, 2.0, 4.0, 5.0, 6.0, 8.0, 10, 20, 40, 50, 60, 80, and 100 $\mu$M from 1 to 24. Inset: variation of fluorescence intensity of 5.0 $\mu$M probe **1** with $Hg^{2+}$ concentration ($\lambda_{ex}$ = 520 nm; $\lambda_{em}$ = 586 nm).

## RESULTS AND DISCUSSION

**Spectral Characteristics of Probe 1.** Figure 1 shows a graph depicting the variation in the fluorescence spectrum of probe **1** after adding different concentrations of mercury ions in Tris−HCl buffer ($CH_3CH_2OH/H_2O$, 1:1, v/v, pH 7.24). As illustrated in Figure 1, probe **1** emitted a very weak fluorescence when $Hg^{2+}$ was not added. As the concentration of $Hg^{2+}$ was increased, probe **1** exhibited enhanced fluorescence. When excess $Hg^{2+}$ was added, the probe demonstrated a 52 times fluorescence increase at 586 nm. The experiment was based on these results to determine the concentration of mercury ions.

In order to explore the sensing mechanism of probe **1** toward $Hg^{2+}$, the variation of the absorption spectrum of probe **1** with the gradual addition of mercury ions was recorded (Figure 2). As demonstrated in Figure 2 the UV−visible absorption spectrum of probe **1** showed a weak absorbance at 565 nm before the addition of mercury ions, which could be ascribed to the presence of the partial ring-opened structure of the spirolactam unit of probe **1**. With the increment of $Hg^{2+}$, probe **1** showed a gradual increase in absorption at 565 nm. When the $Hg^{2+}$ concentration was 50 $\mu$M, the absorbance reached the maximum value. Meanwhile, the solution color change of probe **1** from colorless to pink after the addition of $Hg^{2+}$ could be seen by the naked eye. The possible reason for absorption intensity enhancement at 565 nm was that the ring of the spirolactam structure of probe **1** opened upon the addition of mercury ions. The UV−visible absorption spectroscopy results also indicated that probe **1** interacted with $Hg^{2+}$. Furthermore, a chemical shift of 64.23 ppm in the $^{13}C$ NMR spectrum of probe **1** corresponded to the characteristic chemical shift value of the spirocyclic carbon, which also indicated that probe **1** existed in the spirolactam form before the addition of $Hg^{2+}$.

**Principle of Operation.** To explore the linear correlation between the fluorescence intensity of probe **1** and mercury ions, the fluorescence intensity of probe **1** was studied after the addition of various concentrations of $Hg^{2+}$. The fluorescence intensity of probe **1** at 580 nm linearly depended on the $Hg^{2+}$ concentration when the $Hg^{2+}$ concentration was varied from $8.0 \times 10^{-8}$ to $1.0 \times 10^{-5}$ mol $L^{-1}$ (Figure 3). The linear regression equation used was $F = 25.1293 + 25.1931 \times 10^6 \times C$ ($r$ = 0.9949); here, $F$ is the fluorescence intensity, $C$ represents the concentration of $Hg^{2+}$, and $r$ is the linear correlation coefficient. The detection limit was estimated to be $3.0 \times 10^{-8}$ M based on $3S_B/m$ (where $S_B$ is the standard deviation of 10 blank measurements and $m$ is the slope of the linear regression equation),[49,50] which was more sensitive than that of formerly developed $Hg^{2+}$ fluorescent probes.[26−29] Moreover, according to the UV−vis titration profile in Figure 2, the absorbance of probe **1** at 565 nm increased linearly with the change of the $Hg^{2+}$ concentration of $8.0 \times 10^{-8}$ to $2.0 \times 10^{-5}$ mol $L^{-1}$ (Figure S1, Supporting Information). The linear regression equation used was $A = 0.0569 + 0.1253 \times 10^6 \times C$ ($r$ = 0.9975), where $A$ is the absorbance, $C$ represents the concentration of $Hg^{2+}$, and $r$ is the linear correlation


https://doi.org/10.1021/acsomega.2c03336
ACS Omega 2022, 7, 29236−29245

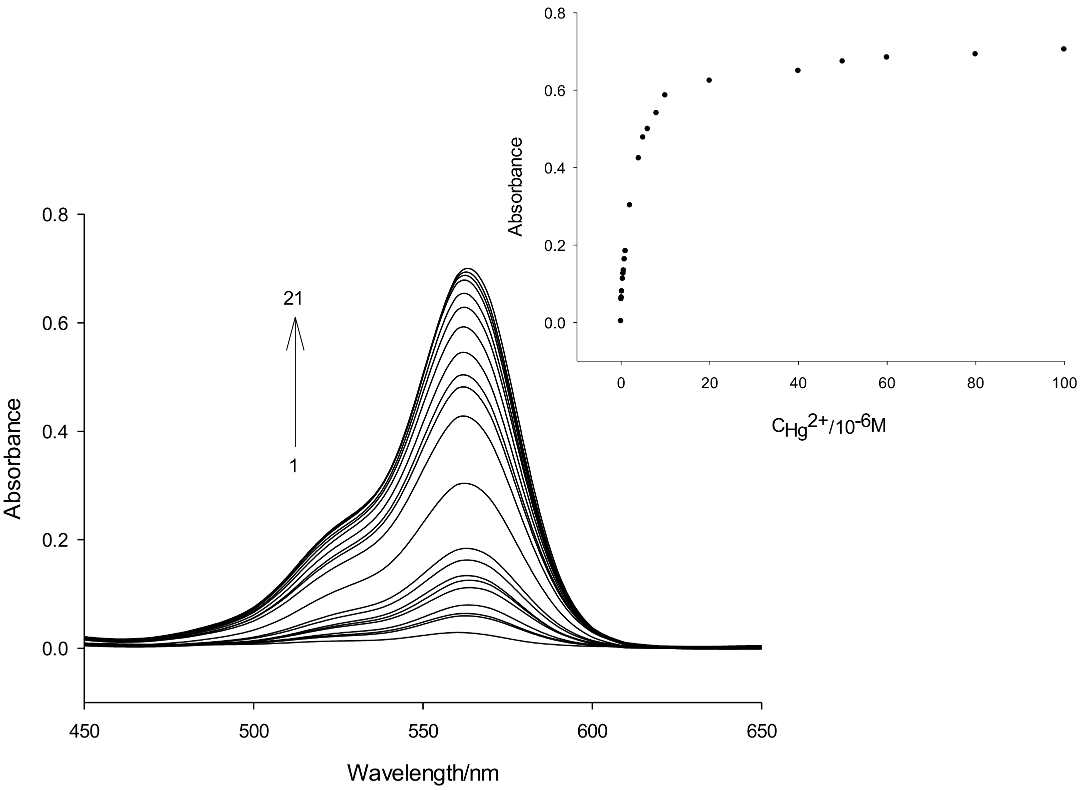


**Figure 2.** UV−vis spectra of 5.0 $\mu$M probe **1** with the gradual addition of $Hg^{2+}$: 0, 0.08, 0.10, 0.20, 0.40, 0.50, 0.60, 0.80, 1.0, 2.0, 4.0, 5.0, 6.0, 8.0, 10, 20, 40, 50, 60, 80, and 100 $\mu$M from 1 to 21. Inset: the variation of absorbance of 5.0 $\mu$M probe 1 with $Hg^{2+}$ concentration.

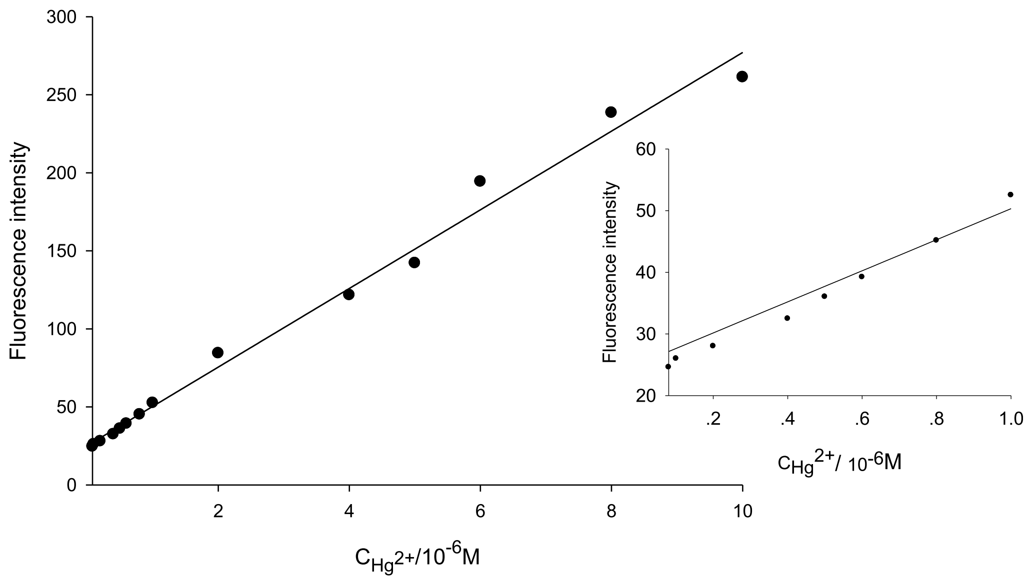


**Figure 3.** Calibration curve between the fluorescence intensity of 5.0 $\mu$M probe **1** and the concentration of mercury ions. Inset: plot of fluorescence intensity of 5.0 $\mu$M probe **1** as a function of $Hg^{2+}$ concentration in the range of 0.08−1.0 $\mu$M.

coefficient. Moreover, the detection limit was found to be 4.8 $\times 10^{-8}$ mol $L^{-1}$ based on $3S_B/m$ (where $S_B$ is the standard deviation of 10 blank measurements and $m$ is the slope of the linear regression equation).[39]

In addition, we also confirmed the stoichiometry of probe **1** with mercury ions by using Job's plot (Figure 4). When the molar fraction of the amount of $Hg^{2+}$ was close to 0.5, the absorbance of probe **1** reached a maximum, indicating that probe **1** coordinated with $Hg^{2+}$ through a 1:1 stoichiometry. Based on the alteration in the absorption spectrum of probe **1** in the absence and presence of mercury ions and the coordination stoichiometry between probe **1** and $Hg^{2+}$, we proposed a possible structural model for the formation of complexes of probe **1** and mercury ions (Scheme 2). To further support the hypothesis, the NMR titration of probe **1** in the presence of $Hg^{2+}$ was carried out (Figure S2, Supporting Information). $Hg^{2+}$ is a heavy metal ion and could influence the proton signals near the $Hg^{2+}$ binding site.[51] From Figure



https://doi.org/10.1021/acsomega.2c03336
ACS Omega 2022, 7, 29236−29245

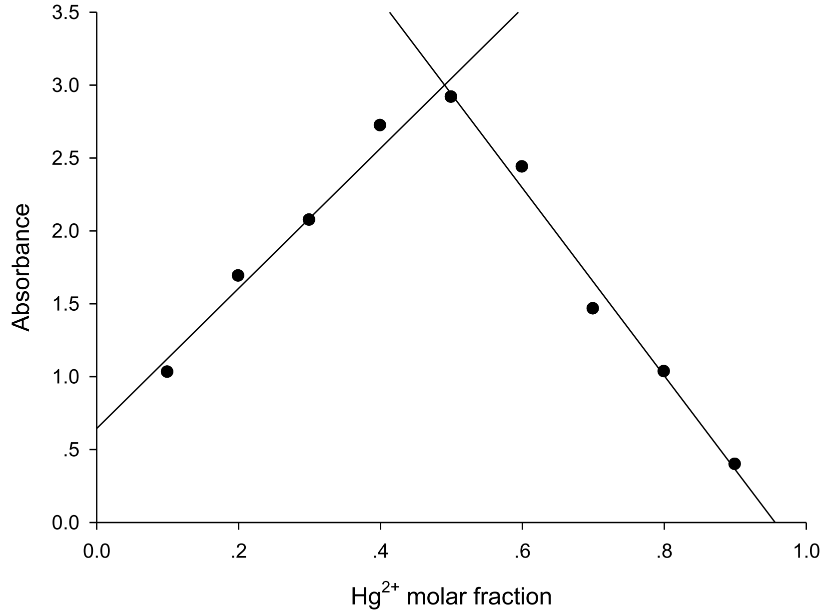


**Figure 4.** Job's plot for confirming the stoichiometry of probe **1** and $Hg^{2+}$ in the $CH_3CH_2OH/H_2O$ (1:1, v/v) solution. The whole concentration of probe **1** and $Hg^{2+}$ was 40 $\mu$M.

**Scheme 2. Likely Complexation Style between the Proposed Probe and $Hg^{2+}$**

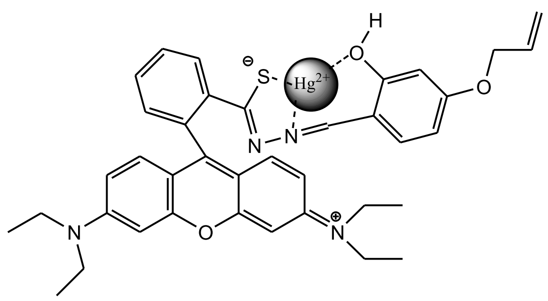

S2, the $^1$H NMR signal of $H_a$ belonging to probe **1** was shifted to the upfield in the presence of $Hg^{2+}$, which demonstrated the binding between the oxygen atom of the hydroxyl group and $Hg^{2+}$. As displayed in Figure S2, the $^1$H NMR signal of $H_b$ in probe **1** also shifted upfield after the addition of $Hg^{2+}$, which illustrated the coordination between the nitrogen atom of the group (−CH═N−) and $Hg^{2+}$. The result of NMR titration experiment further confirmed the coordination mode between the probe and $Hg^{2+}$.

**Effect of pH.** For obtaining information about the pH effect, the fluorescence intensity changes of probe **1** before and after adding $Hg^{2+}$ are investigated in various pH conditions (Figure 5). As exhibited in Figure 5, the fluorescence intensity of probe **1** is substantially unchanged in the range of pH 4.50

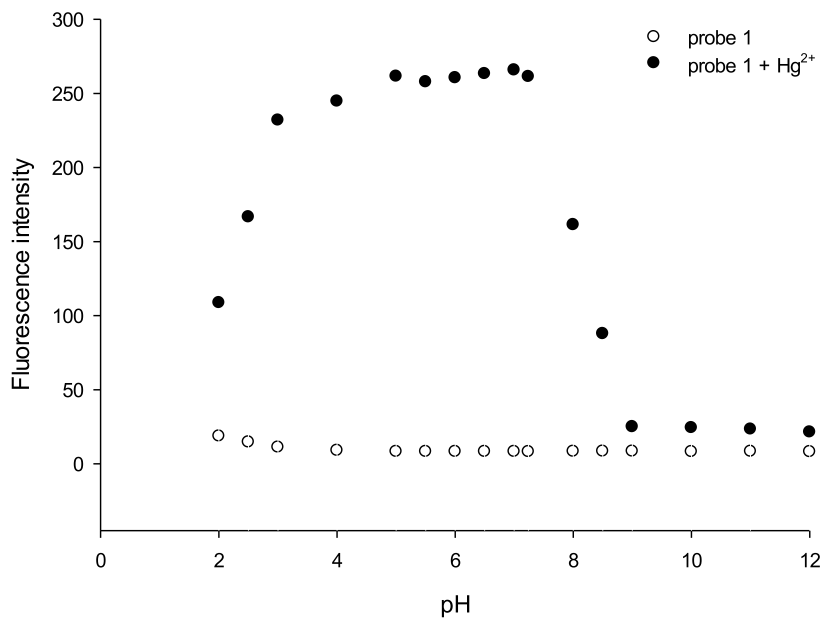


**Figure 5.** Fluorescence intensity variation of 5.0 $\mu$M probe **1** with pH before (open circles) and after (solid circles) adding $Hg^{2+}$.


https://doi.org/10.1021/acsomega.2c03336
ACS Omega 2022, 7, 29236−29245

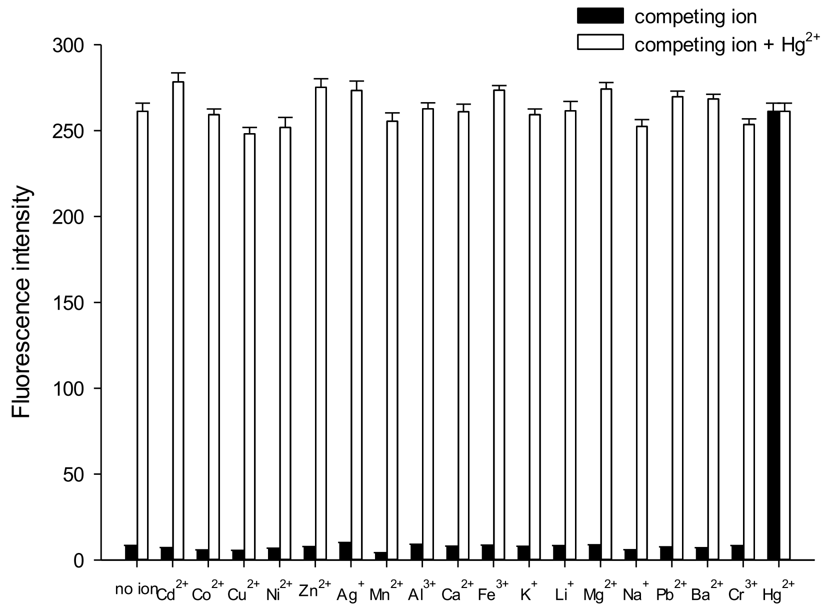


**Figure 6.** Metal-ion selectivity of 5.0 $\mu$M probe **1**. The concentration of ions was $1.0 \times 10^{-5}$ M for $Hg^{2+}$, $Co^{2+}$, $Cu^{2+}$, $Ni^{2+}$, and $Mn^{2+}$ and $1.0 \times 10^{-4}$ M for all other ions. Black bars: various metal ions were provided. White bars: various metal ions in the presence of $Hg^{2+}$ were provided.

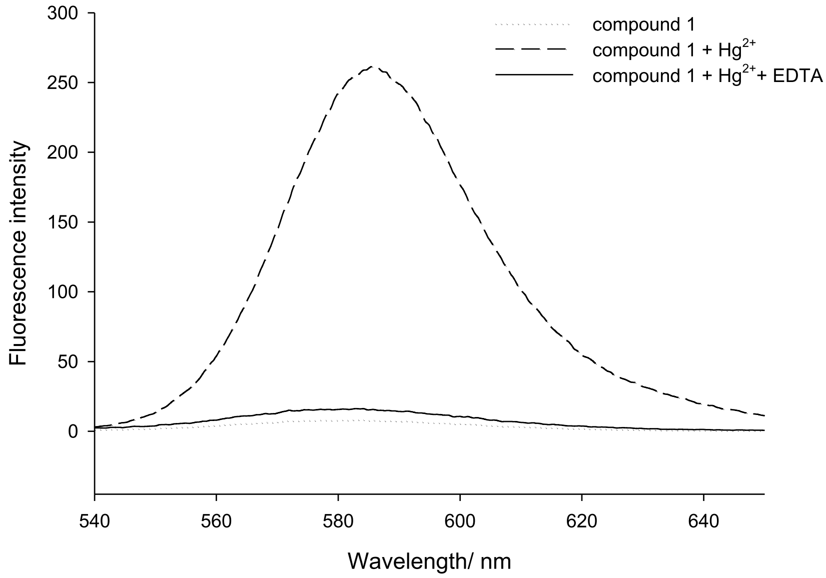


**Figure 7.** Reversibility of probe **1** for $Hg^{2+}$ in Tris−HCl buffer ($CH_3CH_2OH/H_2O$, 1:1, v/v, pH 7.24). ···:5.0 $\mu$M probe **1**; −:5.0 $\mu$M probe **1** with 10 $\mu$M $Hg^{2+}$; —:5.0 $\mu$M probe **1** with 10 $\mu$M $Hg^{2+}$; and following the addition of 40 $\mu$M EDTA 2Na.

to 12.00. However, in the presence of $Hg^{2+}$, the probe exhibited a strong fluorescence in the range of 4.50−8.50. The above results demonstrated that the fluorescent probe was not affected in the pH range of 4.50−8.50 and thus could be exploited to sense $Hg^{2+}$ in the actual samples. When the pH was less than 4.50, probe **1** emitted enhanced fluorescence with reduced pH values, which could be attributed to the ring-opened structure of probe **1** under acidic conditions. Considering the response speed, sensitivity, and practical application, the pH 7.24 Tris−HCl buffer was used in this experiment.

**Selectivity.** In order to ensure that probe **1** could be used in a wide variety of environments, we examined the selectivity of probe **1** for $Hg^{2+}$ (Figure 6). It can be found from the black histogram in Figure 6 that the solution of $Li^+$, $Na^+$, $K^+$, $Mg^{2+}$, $Ca^{2+}$, $Fe^{3+}$, $Al^{3+}$, $Cd^{2+}$, $Zn^{2+}$, $Ag^+$, $Mg^{2+}$, $Pb^{2+}$, $Ba^{2+}$, and $Cr^{3+}$ ions had almost no effect on the fluorescence intensity of probe **1** at a concentration of 10 times the $Hg^{2+}$ concentration. In addition, when the concentrations of $Cu^{2+}$, $Co^{2+}$, $Ni^{2+}$, $Mn^{2+}$, and $Hg^{2+}$ were equal, probe **1** displayed a notable fluorescence increase only upon adding $Hg^{2+}$. The color change, fluorescence change, and UV−vis response of the probe in the absence and presence of those different ions mentioned above were also studied (Figure S3, Supporting Information). From Figures 6 and S3, the probe showed high selectivity for $Hg^{2+}$ by fluorometry. However, the detection of $Hg^{2+}$ was interfered by $Cu^{2+}$ by ultraviolet−visible absorption spectrometry. Moreover, competition experiments were executed in which the developed probe was used to sense $Hg^{2+}$ ($1.0 \times 10^{-5}$ mol $L^{-1}$) in the coexistence solution of $Hg^{2+}$ and other metal ions (white histogram in Figure 6). The experimental results showed that the relative error of usual


https://doi.org/10.1021/acsomega.2c03336
ACS Omega 2022, 7, 29236−29245

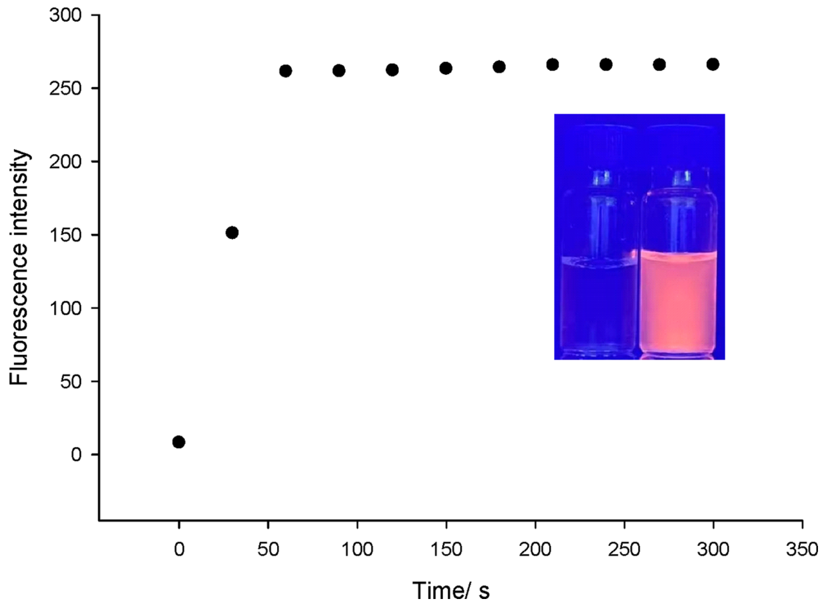


**Figure 8.** Time response of probe **1** (5.0 $\mu$M) for 10 $\mu$M $Hg^{2+}$. Time points are 0, 30, 60, 90, 120, 150, 180, 210, 240, 270, and 300 s; $\lambda_{ex}$ = 520 nm. Inset: visual fluorescence color of probe **1** (5.0 $\mu$M) in the absence (left) and presence (right) of $Hg^{2+}$ for 60 s (UV lamp, 365 nm).

interference including alkaline earth, alkali, and transition-metal ions was lower than ±5%, which was thought to be acceptable. These experiments demonstrated that the coexistence of different metal cations and mercury ions did not affect the determination of $Hg^{2+}$, making the probe more likely to be used to determine actual samples.

For comparison, the complexation study with $Hg^{2+}$ had been carried out using compound **2** (Figure S4, Supporting Information) or compound **3** (Figure S5, Supporting Information) in Tris−HCl buffer ($CH_3CH_2OH/H_2O$, 1:1, v/v, pH 7.24). As demonstrated in Figure S4, in Tris−HCl buffer ($CH_3CH_2OH/H_2O$, 1:1, v/v, pH 7.24), compound 2 showed fluorescence enhancement only in the presence of $Cu^{2+}$. From Figure S5, compound **3** demonstrated a strong fluorescence increase and a pink color only in the presence of $Cu^{2+}$ or $Hg^{2+}$ (Figure S5 in the revised Supporting Information). Thus, probe **1** possessed higher selectivity for $Hg^{2+}$ compared with compound **2** and compound **3**.

**Reversibility and Response Time.** It was apparent to all that reversibility is a significant factor to prepare an excellent chemical sensor. We tested the reversibility of probe **1** by adding an EDTA solution (Figure 7). As demonstrated in Figure 7, the fluorescence intensity of probe **1** drastically increased after providing mercury ions, and the solution color transformed from colorlessness to pink. However, after the EDTA solution was added to the above pink solution, the fluorescence intensity decreased rapidly, and the solution color was altered from pink to colorlessness. These experimental consequences explained that the complexation process of probe **1** and $Hg^{2+}$ was reversible.

At the same time, we also studied the time response of probes to mercury ions (Figure 8). $Hg^{2+}$ ($1.0 \times 10^{-5}$ mol $L^{-1}$) were added to probe **1** solution, and the change in fluorescence intensity from 0.0 to 5.0 min was recorded to examine the time response of probe **1** for $Hg^{2+}$. From Figure 8, it can be observed that the complexation speed of probe **1** and $Hg^{2+}$ was very rapid, and the fluorescence intensity could reach the maximum within 60 s. The response time of the proposed probe for $Hg^{2+}$ was shorter than that of formerly reported fluorescent probes for $Hg^{2+}$.[20−23] Therefore, the fluorescent probe would be utilized for real-time $Hg^{2+}$ detection.

Compared with other probes for $Hg^{2+}$ based on rhodamine derivatives (as displayed in Table S1, Supporting Information), this probe possessed many advantages including high sensitivity and specificity, fast response time, a wide pH working range, and so forth.

**Preliminary Analytical Application.** For verifying the application of probe **1** in actual sample analysis, probe **1** was utilized for the sensing of mercury ions in tap water and river water samples. The river water and tap water were directly used after being filtered by a 0.45 $\mu$m filter. The river water and tap water were measured by probe **1** for mercury ion content, which contained no $Hg^{2+}$, and then the standard solutions of different concentrations of $Hg^{2+}$ were separately added for the determination of the recovery rate (Table 1). As found from Table 1, the fluorescent probe has a satisfactory determination result of $Hg^{2+}$ recovery rate in the tap water and river water. Thus, the probe could be effectively used to sense $Hg^{2+}$ in the actual samples.

**Table 1. Sensing $Hg^{2+}$ in Tap and River Water Samples with Probe 1**

| | sample | $Hg^{2+}$ spiked (mol $L^{-1}$) | $Hg^{2+}$ recovered (mol $L^{-1}$) | recovery (%) |
|---|---|---|---|---|
| river water | 1 | 0 | not detected | |
| | 2 | $5.00 \times 10^{-6}$ | $(5.15^{a} \pm 0.10^{b}) \times 10^{-6}$ | 103.0 |
| | 3 | $1.00 \times 10^{-5}$ | $(1.02^{a} \pm 0.02^{b}) \times 10^{-5}$ | 102.0 |
| tap water | 1 | 0 | not detected | |
| | 2 | $5.00 \times 10^{-6}$ | $(5.18^{a} \pm 0.12^{b}) \times 10^{-6}$ | 103.6 |
| | 3 | $1.00 \times 10^{-5}$ | $(0.98^{a} \pm 0.03^{b}) \times 10^{-5}$ | 98.0 |

[a]Mean values of three determinations. [b]Standard deviation.


https://doi.org/10.1021/acsomega.2c03336
ACS Omega 2022, 7, 29236−29245

We also conducted a bio-imaging application research of probe **1**. To assess the biocompatibility of probe **1**, we performed a cytotoxicity assay using the MTT colorimetric assay (Figure S6, Supporting Information). From Figure S1, the cell viability of A549 cells was found to be higher than 90% when probe **1** was present, indicating that probe **1** was almost not cytotoxic. Next, we verified whether probe **1** could be employed for sensing $Hg^{2+}$ in living cells by laser confocal fluorescence imaging experiments (Figure 9). As can be seen from Figure 9a, after culturing A549 cells in medium containing probe **1** (5.0 $\mu$M) for 30 min, the cells showed substantially no fluorescence. However, when A549 cells were cultured for 30 min with 1.0 $\mu$M $Hg^{2+}$ under the same conditions, the cells exhibited a strong fluorescence (Figure 9d). According to the research results, probe **1** could be applied to fluorescence imaging of $Hg^{2+}$ in living cells.

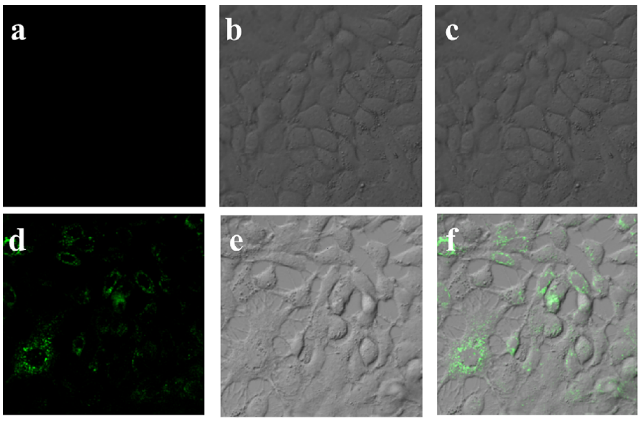


**Figure 9.** Images of A549 cells incubated with the developed probe **1**. (a) Fluorescence image of A549 cells attached to 5.0 $\mu$M probe **1** for 30 min at 37 °C; (b) bright-field transmission image of cells demonstrated in (a); (c) overlap image of (a,b); (d) fluorescence image of A549 cells attached to 5.0 $\mu$M probe **1** for 30 min, washed three times, and further treated with 1.0 $\mu$M $Hg^{2+}$ for 30 min; (e) bright-field transmission image of cells displayed in (d); and (f) overlap image of (d,e).

## CONCLUSIONS

On the whole, a new fluorescent probe has been planned and prepared to quantify $Hg^{2+}$, which used rhodamine as the fluorophore. After providing $Hg^{2+}$, the probe displayed a strong fluorescence emission and a pink color due to its open-cycle structure of the corresponding spirolactam via a reversible coordination. The fluorescent probe exhibited excellent sensing abilities, including excellent sensitivity and specificity, rapid response, a wide pH working range, and so forth. The fluorescent probe had been applied to sense $Hg^{2+}$ in both tap and river water samples and demonstrated acceptable consequences. Furthermore, the probe also demonstrated superior biocompatibility, which permitted us to obtain fluorescence imaging of $Hg^{2+}$ in A549 cells.

## EXPERIMENTAL SECTION

**Materials and Instruments.** Lawesson's reagent (97%) and allyl bromide were purchased from Aldrich. Rhodamine B and hydrazine monohydrate (85%) were bought from Shanghai Sinopharm Group Company. Before toluene was utilized, it was freshly distilled through adding sodium. Unless otherwise stated, other chemical reagents used in this work were of analytical grade and could be applied directly. Water used in all assays was ultrapure water.

UV−vis and fluorescence spectra were measured on a UV-2600 spectrometer and a Hitachi F-7000 spectrophotometer, respectively. A Bruker DRX-500 NMR spectrometer was utilized to measure the NMR spectra. Fluorescence images of living cells were acquired through an Olympus FV1200-MPE multiphoton laser scanning confocal microscope with a 40× objective lens. The pH of the solution was measured with a Mettler Toledo Delta 320 pH meter. SigmaPlot software was used to perform the data processing.

**Syntheses.** The method of preparation of fluorescent probe **1** is demonstrated in Scheme 1. During the process, product **2** was obtained through the interaction of hydrazine monohydrate (85%) and rhodamine B, as reported in the previous literature.[52] Compound **3** was obtained by the chemical reaction between Lawesson's reagent and compound **2** following an earlier developed method.[52] 4-Formyl-3-hydroxyphenyl allyl ether (compound **4**) was synthesized from 2,4-dihydroxybenzaldehyde and allyl bromide following a formerly developed procedure.[53]

**Synthesis of Compound 1.** Compound **3** (0.19 g, 0.40 mmol) and compound **4** (0.096 g, 0.54 mmol) were put in 50 mL $CH_3CH_2OH$. The mixture was warmed to refluxing for 12 h. After the solvents were cleaned in decompression, purification of the crude product was done through column chromatography ($CH_3COOCH_2CH_3$/petroleum ether = 1:10, v/v) to produce probe **1** (0.19 g, 75%) as a pale yellow solid. $^1H$ NMR (500 MHz, $CDCl_3$): $\delta$(ppm) 11.50 (1H, s), 8.62 (1H, s), 8.09 (1H, dd, $J$ = 5.8 Hz, 3.2 Hz), 7.41 (2H, dd, $J$ = 5.8 Hz, 3.2 Hz), 7.19 (1H, d, $J$ = 8.5 Hz), 7.13−7.11 (1H, m), 6.74 (2H, d, $J$ = 8.8 Hz), 6.49−6.42 (2H, m), 6.32−6.27 (4H, m), 6.05−5.97 (1H, m), 5.39 (1H, dd, $J$ = 17.2 Hz, 1.4 Hz), 5.27 (1H, dd, $J$ = 10.5 Hz, 1.2 Hz), 4.51 (2H, d, $J$ = 5.3 Hz), 3.31 (8H, q, $J$ = 7.0 Hz), 1.14 (12H, t, $J$ = 7.0 Hz) (Figure S7, Supporting Information). $^{13}C$ NMR (125 MHz, $CDCl_3$): $\delta$(ppm) 170.13, 162.38, 161.97, 161.07, 155.13, 151.93, 148.33, 135.19, 133.02, 132.67, 132.16, 130.11, 127.91, 127.12, 122.21, 117.99, 111.75, 110.17, 108.28, 107.63, 101.92, 97.53, 68.83, 64.23, 44.37, 12.60 (Figure S8, Supporting Information). MS (ESI) $m/z$: 633.2902 $(M + H)^+$ (Figure S9, Supporting Information).

**Measurement Procedures of Fluorescence Intensity.** The preparation of $1.0 \times 10^{-5}$ mol $L^{-1}$ probe **1** was done by adding the needed quantity of probe **1** to $CH_3CH_2OH$. $8 \times 10^{-7}$−$1.0 \times 10^{-3}$ mol $L^{-1}$ $Hg^{2+}$ stock solution was obtained by gradually diluting $1.0 \times 10^{-2}$ mol $L^{-1}$ mercury nitrate solution with 0.05 mol $L^{-1}$ Tris−HCl buffer (pH, 7.24). The 0.05 mol $L^{-1}$ Tris−HCl solution was adjusted by adding HCl or NaOH solution to obtain a range of pH buffer solutions. 12.50 mL of $1.0 \times 10^{-5}$ mol $L^{-1}$ probe **1** and 2.50 mL of different concentrations of $Hg^{2+}$ solution were put into a 25 mL volumetric flask and then it was made up to 25 mL using 0.05 mol $L^{-1}$ Tris−HCl buffer. A solution containing $5 \times 10^{-6}$ mol $L^{-1}$ probe **1** and $8 \times 10^{-8}$−$1 \times 10^{-4}$ mol $L^{-1}$ $Hg^{2+}$ was obtained. The same procedure without adding $Hg^{2+}$ was used to obtain the blank solution of probe **1**.

All solutions were kept at 4 °C in the dark. The excited wavelength was 520 nm, and both the entrance and exit slits were of 2.5 nm, and the fluorescence intensity was recorded in the range of 540−650 nm.


https://doi.org/10.1021/acsomega.2c03336
ACS Omega 2022, 7, 29236−29245

## ■ ASSOCIATED CONTENT

### Supporting Information

The Supporting Information is available free of charge at https://pubs.acs.org/doi/10.1021/acsomega.2c03336.

$^1$H NMR spectra of probe **1** before and after adding $Hg^{2+}$; absorbance of probe **1** at 565 nm with different metal ions; fluorescence and color changes of probe **1** with different metal ions; absorbance and fluorescence of compound **2** at 586 nm with different metal ions; fluorescence and color changes of compound **2** with different metal ions; absorbance and fluorescence of compound **3** at 586 nm with different metal ions; fluorescence and color changes of compound **3** with different metal ions; comparison of fluorescent probes for determination of $Hg^{2+}$ based on rhodamine derivatives; assay of A549 cells in the presence of different concentrations of probe **1** (0, 2, 4, 8, and 16 $\mu$M) for 24 h at 37 °C; $^1$H and $^{13}$C NMR spectra of compound **1**; and ESI−MS spectra of compounds **1** (PDF)

## ■ AUTHOR INFORMATION


### Corresponding Authors

**Qiujuan Ma** − *School of Pharmacology, Henan University of Chinese Medicine, Zhengzhou 450046, P. R. China;* orcid.org/0000-0001-9785-2733; Email: maqiujuan104@126.com

**Yang Geng** − *Department of Pharmacy, Zhengzhou Railway Vocational and Technical College, Zhengzhou 451460, P. R. China;* Email: gengyang0001@163.com

### Authors

**Nannan Zhu** − *School of Pharmacology, Henan University of Chinese Medicine, Zhengzhou 450046, P. R. China*

**Junhong Xu** − *Department of Dynamical Engineering, North China University of Water Resources and Electric Power, Zhengzhou 450011, P. R. China*

**Linke Li** − *School of Pharmacology, Henan University of Chinese Medicine, Zhengzhou 450046, P. R. China*

**Shuzhen Liu** − *School of Pharmacology, Henan University of Chinese Medicine, Zhengzhou 450046, P. R. China*

**Shuangyu Liu** − *School of Pharmacology, Henan University of Chinese Medicine, Zhengzhou 450046, P. R. China*

**Gege Wang** − *School of Pharmacology, Henan University of Chinese Medicine, Zhengzhou 450046, P. R. China*

Complete contact information is available at: https://pubs.acs.org/10.1021/acsomega.2c03336


### Notes

The authors declare no competing financial interest.

## ■ ACKNOWLEDGMENTS

This work was supported by the National Natural Science Foundation of China (grant no. 21807027), the Zhongjing Scholars Research Funding of Henan University of Chinese Medicine, and the Graduate Innovation Fund of the Henan College of Chinese Medicine (2021KYCX051).

## ■ REFERENCES


(1) Chen, X.; Pradhan, T.; Wang, F.; Kim, J. S.; Yoon, J. Fluorescent chemosensors based on spiroring-opening of xanthenes and related derivatives. *Chem. Rev.* **2012**, *112*, 1910−1956.

(2) Li, X.; Gao, X.; Shi, W.; Ma, H. Design strategies for water-soluble small molecular chromogenic and fluorogenic probes. *Chem. Rev.* **2014**, *114*, 590−659.

(3) She, M.; Wang, Z.; Chen, J.; Li, Q.; Liu, P.; Chen, F.; Zhang, S.; Li, J. Design strategy and recent progress of fluorescent probe for noble metal ions (Ag, Au, Pd, and Pt). *Coord. Chem. Rev.* **2021**, *432*, 213712.

(4) Tchounwou, P. B.; Ayensu, W. K.; Ninashvili, N.; Sutton, D. Review: Environmental exposure to mercury and its toxicopathologic implications for public health. *Environ. Toxicol.* **2003**, *18*, 149−175.

(5) Counter, S. A.; Buchanan, L. H. Mercury exposure in children: a review. *Toxicol. Appl. Pharmacol.* **2004**, *198*, 209−230.

(6) Harris, H. H.; Pickering, I. J.; George, G. N. The chemical form of mercury in fish. *Science* **2003**, *301*, 1203.

(7) Weiss, B. Why methylmercury remains a conundrum 50 years after Minamata. *Toxicol. Sci.* **2007**, *97*, 223−225.

(8) Zahir, F.; Rizwi, S. J.; Haq, S. K.; Khan, R. H. Low dose mercury toxicity and human health. *Environ. Toxicol. Pharmacol.* **2005**, *20*, 351−360.

(9) Díez, S. Human health effects of methylmercury exposure. *Rev. Environ. Contam. Toxicol.* **2009**, *198*, 111−132.

(10) *Mercury Update: Impact on Fish Advisories. EPA Fact Sheet EPA-823-F-01-011*; EPA, Office of Water: Washington, DC, 2001.

(11) Zhou, D. B.; Xiao, Y. B.; Han, F.; Lv, Y. N.; Ding, L.; Song, W.; Liu, Y. X.; Zheng, P.; Chen, D. Magnetic solid-phase extraction based on sulfur-functionalized magnetic metal-organic frameworks for the determination of methylmercury and inorganic mercury in water and fish samples. *J. Chromatogr. A* **2021**, *1654*, 462465.

(12) Chen, D. Y.; Lu, L.; Zhang, H.; Lu, B.; Feng, J. L.; Zeng, D. Sensitive mercury speciation analysis in water by high-performance liquid chromatography-atomic fluorescence spectrometry coupling with solid-phase extraction. *Anal. Sci.* **2021**, *37*, 1235−1240.

(13) Anthemidis, A. N.; Zachariadis, G. A.; Michos, C. E.; Stratis, J. A. Time-based on-line preconcentration cold vapour generation procedure for ultra-trace mercury determination with inductively coupled plasma atomic emission spectrometry. *Anal. Bioanal. Chem.* **2004**, *379*, 764−769.

(14) Miranda-Andrades, J. R.; Letichevsky, S.; González Larrudé, D. R. G.; Aucelio, R. Q. Photo-generation of mercury cold vapor mediated by graphene quantum dots/$TiO_2$ nanocomposite: on line time-resolved speciation at ultra-trace levels. *Anal. Chim. Acta* **2020**, *1127*, 256−268.

(15) Monisha, K.; Shrivas, T.; Kant, S.; Patel, R.; Devi, N. S.; Dahariya, S.; Pervez, M. K.; Deb, M. K.; Rai, J.; Rai, J. Inkjet-printed paper-based colorimetric sensor coupled with smartphone for determination of mercury ($Hg^{2+}$). *J. Hazard. Mater.* **2021**, *414*, 125440.

(16) Chen, S. Y.; Li, Z.; Li, K.; Yu, X. Q. Small molecular fluorescent probes for the detection of lead, cadmium and mercury ions. *Coord. Chem. Rev.* **2021**, *429*, 213691.

(17) Wang, Y.; Zhang, L.; Han, X.; Zhang, L.; Wang, X.; Chen, L. Fluorescent probe for mercury ion imaging analysis: strategies and applications. *Chem. Eng. J.* **2021**, *406*, 127166.

(18) Yantasee, W.; Lin, Y. H.; Zemanian, T. S.; Fryxell, G. E. Voltammetric detection of lead(II) and mercury(II) using a carbon paste electrode modified with thiol self-assembled monolayer on mesoporous silica (SAMMS). *Analyst* **2003**, *128*, 467−472.

(19) Zhang, J. L.; Zhu, Z. W.; Di, J. W.; Long, Y. M.; Li, W. F.; Tu, Y. F. A sensitive sensor for trace $Hg^{2+}$ determination based on ultrathing-$C_3N_4$ modified glassy carbon electrode. *Electrochim. Acta* **2015**, *186*, 192−200.

(20) Tian, M.; Wang, C.; Ma, Q.; Bai, Y.; Sun, J.; Ding, C. A highly selective fluorescent probe for $Hg^{2+}$ based on a 1,8-naphthalimide derivative. *ACS Omega* **2020**, *5*, 18176−18184.

(21) Huang, L.; Yang, Z.; Zhou, Z.; Li, Y.; Tang, S.; Xiao, W.; Hu, M.; Peng, C.; Chen, Y.; Gu, B.; Li, H. A dual colorimetric and near-infrared fluorescent turn-on probe for $Hg^{2+}$ detection and its applications. *Dyes Pigm.* **2019**, *163*, 118−125.

(22) Xu, J.; Li, H.; Chen, Y.; Yang, B.; Jiao, Q.; Yang, Y.; Zhu, H. L. A novel fluorescent probe for $Hg^{2+}$ detection in a wide pH range and its application in living cell imaging. *Anal. Methods* **2018**, *10*, 5554−5558.

(23) Prabhu, J.; Velmurugan, K.; Nandhakumar, R. A highly selective and sensitive naphthalene-based chemodosimeter for $Hg^{2+}$ ions. *J. Lumin.* **2014**, *145*, 733−736.

(24) Tian, M.; Liu, L.; Li, Y.; Hu, R.; Liu, T.; Liu, H.; Wang, S.; Li, Y. An unusual OFF-ON fluorescence sensor for detecting mercury ions in aqueous media and living cells. *Chem. Commun.* **2014**, *50*, 2055−2057.

(25) Rani, B. K.; John, S. A. Fluorogenic mercury ion sensor based on pyrene-amino mercapto thiadiazole unit. *J. Hazard. Mater.* **2018**, *343*, 98−106.

(26) Bozkurt, E.; Gul, H. I. Selective fluorometric "Turn-off" sensing for $Hg^{2+}$ with pyrazoline compound and its application in real water sample analysis. *Inorg. Chim. Acta* **2020**, *502*, 119288.

(27) Jiang, X. D.; Zhao, J.; Li, Q.; Sun, C. L.; Guan, J.; Sun, G. T.; Xiao, L. J. Synthesis of NIR fluorescent thienyl-containing aza-BODIPY and its application for detection of $Hg^{2+}$: electron transfer by bonding with $Hg^{2+}$. *Dyes Pigm.* **2016**, *125*, 136−141.

(28) Erdemir, S.; Oguz, M.; Malkondu, S. A NIR fluorescent sensor based on thiazoline-isophorone with low cytotoxicity in living cells for $Hg^{2+}$ detection through ICT associated hydrogen bonding effect. *Anal. Chim. Acta* **2022**, *1192*, 339353.

(29) Wu, D.; Ma, M.; Zhang, M.; Xiao, Y.; Yu, H.; Shao, Y.; Zhang, X.; Cheng, Z.; Xiao, Y. $Hg^{2+}$ rhodamine fluorescent probe bearing flexible $\alpha$-amino acid hydrazines and its photoactivation under UV light. *Dyes Pigm.* **2022**, *198*, 110001.

(30) Venkatesan, P.; Thirumalivasan, N.; Wu, S. P. A rhodamine-based chemosensor with diphenylselenium for highly selective fluorescence turn-on detection of Hg2+in vitro and in vivo. *RSC Adv.* **2017**, *7*, 21733−21739.

(31) Rajasekar, M. Recent trends in rhodamine derivatives as fluorescent probes for biomaterial applications. *J. Mol. Struct.* **2021**, *1235*, 130232.

(32) He, H.; Cheng, Z.; Zheng, L.; Zhang, X. Evaluation of fluorescent $Cu^{2+}$ probes: instant sensing, cell permeable recognition and quantitative detection. *Molecules* **2021**, *26*, 512.

(33) Zhu, J. P.; Yeo, J. H.; Bowyer, A. A.; Proschogo, N.; New, E. J. Studies of the labile lead pool using a rhodamine-based fluorescent probe. *Metallomics* **2020**, *12*, 644−648.

(34) Jiang, T. T.; Bian, W. W.; Kan, J. F.; Sun, Y. Y.; Ding, N.; Li, W. J.; Zhou, J. Sensitive and rapid detection of $Cr^{3+}$ in live cells by a red turn-on fluorescent probe. *Spectrochim. Acta, Part A* **2021**, *245*, 118903.

(35) Gao, J.; He, Y. Q.; Chen, Y. C.; Song, D. F.; Zhang, Y. M.; Qi, F.; Guo, Z. J.; He, W. J. Reversible FRET fluorescent probe for ratiometric tracking of endogenous $Fe^{3+}$ in ferroptosis. *Inorg. Chem.* **2020**, *59*, 10920−10927.

(36) Das, S.; Pratim Das, P. P.; Walton, J. W.; Ghoshal, K.; Patra, L.; Bhattacharyya, M. FRET based ratiometric switch for selective sensing of $Al^{3+}$ with bio-imaging in human peripheral blood mononuclear cells. *New J. Chem.* **2021**, *45*, 1853−1862.

(37) Sun, J.; Li, T. R.; Yang, Z. Y. A novel fluorescent probe based on 7,8-benzochromone-3-carbaldehyde-(rhodamine B carbonyl) hydrazone for detection of trivalent cations and $Zn^{2+}$ in different systems. *J. Photochem. Photobiol., A* **2021**, *411*, 113207.

(38) Wu, J. S.; Hwang, I. C.; Kim, K. S.; Kim, J. S. Rhodamine-based $Hg^{2+}$-selective chemodosimeter in aqueous solution: fluorescent OFF−ON. *Org. Lett.* **2007**, *9*, 907−910.

(39) Zheng, H.; Qian, Z. H.; Xu, L.; Yuan, F. F.; Lan, L. D.; Xu, J. G. Switching the recognition preference of rhodamine B spirolactam by replacing one atom: design of rhodamine B thiohydrazide for recognition of Hg(II) in aqueous solution. *Org. Lett.* **2006**, *8*, 859−861.

(40) Wang, Y.; Ding, H.; Zhu, Z.; Fan, C.; Tu, Y.; Liu, G.; Pu, S. Selective rhodamine-based probe for detecting $Hg^{2+}$ and its application as test strips and cell staining. *J. Photochem. Photobiol., A* **2020**, *390*, 112302.

(41) Kan, C.; Shao, X.; Song, F.; Xu, J.; Zhu, J.; Du, L. Bioimaging of a fluorescence rhodamine-based probe for reversible detection of Hg (II) and its application in real water environment. *Microchem. J.* **2019**, *150*, 104142.

(42) Song, F.; Yang, C.; Shao, X.; Du, L.; Zhu, J.; Kan, C. A reversible "turn-off-on" fluorescent probe for real-time visualization of mercury (II) in environmental samples and its biological applications. *Dyes Pigm.* **2019**, *165*, 444−450.

(43) Cicekbilek, F.; Yilmaz, B.; Bayrakci, M.; Gezici, O. An application of a schiff-base type reaction in the synthesis of a new rhodamine-based Hg(II)-sensing agent. *J. Fluoresc.* **2019**, *29*, 1349−1358.

(44) Meng, X.; Li, Z.; Ma, W. A highly sensitivity fluorescent probe based on rhodamine for naked-eye detection of $Hg^{2+}$ in aqueous solution. *Int. J. Environ. Anal. Chem.* **2021**, *0*, 1−11.

(45) Wang, Y.; Ding, H.; Wang, S.; Fan, C.; Tu, Y.; Liu, G.; Pu, S. A ratiometric and colorimetric probe for detecting $Hg^{2+}$ based on naphthalimide-rhodamine and its staining function in cell imaging. *RSC Adv.* **2019**, *9*, 11664−11669.

(46) Gauthama, B. U.; Narayana, B.; Sarojini, B. K.; Suresh, N. K.; Sangappa, Y.; Kudva, A. K.; Satyanarayana, G.; Raghu, S. V. Colorimetric "off-on" fluorescent probe for selective detection of toxic $Hg^{2+}$ based on rhodamine and its application for in-vivo bioimaging. *Microchem. J.* **2021**, *166*, 106233.

(47) Cui, C.; Gao, X.; Jia, X.; Jiao, Y.; Duan, C. A rhodamine B-based turn on fluorescent probe for selective recognition of mercury(II) ions. *Inorg. Chim. Acta* **2021**, *520*, 120285.

(48) Lv, H.; Sun, H. A lysosome-targetable two-photon excited near-infrared fluorescent probe for visualizing hypochlorous acid-involved arthritis and its treatment. *Spectrochim. Acta, Part A* **2021**, *249*, 119326.

(49) Tian, T. J.; Xu, J. H.; Ma, Q. J.; Li, L. K.; Yuan, H. M.; Sun, J. G.; Zhu, N. N.; Liu, S. Z. A novel lysosome-located fluorescent probe for highly selective determination of hydrogen polysulfides based on a naphthalimide derivative. *Spectrochim. Acta, Part A* **2022**, *268*, 120708.

(50) Shen, Y. M.; Zhang, X. Y.; Zhang, Y. Y.; Li, H. T. L.; Dai, C.; Peng, X. J.; Peng, Z.; Xie, Y. T. A fluorescent sensor for fast detection of peroxynitrite by removing of C=N in a benzothiazole derivative. *Anal. Chim. Acta* **2018**, *1014*, 71−76.

(51) McClure, D. S. Spin-orbit interaction in aromatic molecules. *J. Chem. Phys.* **1952**, *20*, 682−686.

(52) Ma, Q. J.; Zhang, X. B.; Zhao, X. H.; Jin, Z.; Mao, G. J.; Shen, G. L.; Yu, R. Q. A highly selective fluorescent probe for $Hg^{2+}$ based on a rhodamine-coumarin conjugate. *Anal. Chim. Acta* **2010**, *663*, 85−90.

(53) Ma, Q. J.; Zhang, X. B.; Zhao, X. H.; Gong, Y. J.; Tang, J.; Shen, G. L.; Yu, R. Q. A ratiometric fluorescent sensor for zinc ions based on covalently immobilized derivative of benzoxazole. *Spectrochim. Acta, Part A* **2009**, *73*, 687−693.